Journal of Petroleum Science and Engineering 145 (2016) 436–443

Contents lists available at ScienceDirect

Journal of Petroleum Science and Engineering

journal homepage: www.elsevier.com/locate/petrol

Rock physics modelling of acoustic velocities for heavy oil sand

Junxin Guo, Xuehui Han *

School of Geoscience, China University of Petroleum (East China), Qingdao 266580, China

ARTICLE INFO

Article history:
Received 12 December 2015
Received in revised form
19 May 2016
Accepted 23 May 2016
Available online 25 May 2016

Keywords:
Acoustic velocity
Heavy oil sand
Oil distribution
Rock physics modelling

ABSTRACT

The rock physics models for the acoustic velocities of the heavy oil sand with different oil distributions are proposed in this paper. The heavy oil distributions are classified into three primary types, based on which the corresponding acoustic velocity models are given. For the first type, the heavy oil is detached from the sand grains, for which the Hertz-Mindlin- Hashin-Shtrikman (HMHS) model can be used. In the second type, a continuous matrix is formed by the heavy oil and the sand grains float inside the matrix. The Hashin- Shtrikman (HS) lower bound gives good estimation results under this condition. For the third type, the heavy oil cements the sand grains at the grain contacts. The modified Contact Cement Theory (CCT) can describe this cementation effect well. To validate the proposed models, we analyzed the heavy oil sand data from Xinjiang Oil Field of China. The heavy oil distribution is obtained and the corresponding model is selected to estimate the acoustic velocities. The results show that it can predict the measured data well. Furthermore, we also compare the responses of the acoustic velocities for the heavy oil sand with different oil distributions. It reveals that different heavy oil distribution results in different acoustic velocities responses. The heavy oil distribution can thus be obtained by matching the measured data with the results estimated by the models. The model that match the data best implies the primary oil distribution. Many properties of the sand can then be estimated from the heavy oil distribution, such as the strength and permeability of the sand.

1. Introduction

The heavy oil sand is an important type of hydrocarbon reservoirs, which contributes a large amount of the world's reserves of oil and gas. Different from the oils in the conventional reservoirs, the heavy oils often exhibit the property of high viscosity. This results in the difficulties of using the conventional technologies to produce the heavy oil. In order to enhance the heavy oil production, a variety of methods have been proposed (Speight, 2013). These methods focus on lowering the viscosity of the heavy oil through the injection of the chemical solvents or the heat. Among them, thermal recovery has been proved to be the most efficient method. During the thermal recovery, monitoring the physical property changes of heavy oil sands is of great importance to the improvement of the recovery efficiency. For this purpose, the geophysical methods, such as 4D seismic technology and sonic well logging, are usually applied (Gurevich et al., 2007). The analysis of the acquired seismic or logging data provides the information needed for the operation of thermal recovery. However, most current analyses are based on the qualitative analysis and the information contained in the data are not fully extracted, which is due to the complex properties of the heavy oil sand. Hence, it is essential to carry out the quantitative analysis of the acquired seismic and logging data. To this end, building the rock physics models which connect the measured geophysical parameters with the physical properties of the heavy oil sand is necessary. In order to do so, it is most important to establish the relationship between the fundamental geophysical parameter, i.e., the acoustic velocities, with the physical properties of the heavy oil sand.

The properties of the heavy oil are controlled by the temperature (Han et al., 2006). Depending on the different properties of the heavy oil at varying temperatures, the acoustic velocities of the heavy oil sand also changes. At low temperature, the heavy oil behaves like the elastic solid. Under this condition, the effective elastic properties of the heavy oil sand are dominated by the heavy oil distributions (Han et al., 2007). Then it transfers to the quasi-solid phase with the increasing temperature. At this phase, the heavy oil exhibits the viscoelastic properties. It means that it behaves like the fluid in the low frequencies, but almost like the elastic solid in the high frequencies. In this case, the acoustic velocities of the heavy oil sand are frequency dependent and the intrinsic energy dissipations can be observed (Wolf et al., 2006; Han et al., 2008). The heavy oil distribution also plays an important role on the acoustic velocities. When the temperature continues to increase, the heavy oil will transfer to the fluid phase for which Gassmann equations (Gassmann, 1951) can be applied to

* Corresponding author.
E-mail address: hanxuehui_rock@163.com (X. Han).

http://dx.doi.org/10.1016/j.petrol.2016.05.028
0920-4105/

estimate its effects on the acoustic velocities of the heavy oil sand.

Up until now, a number of rock physics models have been proposed for the elastic properties and acoustic velocities of the heavy oil sand in the low and intermediate temperatures. Marion and Nur (1991) and Das and Batzle (2008) applied the Hashin-Shtrikman (HS) lower bounds and the averaging methods to predict elastic moduli for the heavy oil sand, whose results agree with the experimental data well. Gurevich et al. (2007, 2008) combined the HS bounds with the Coherent Potential Approximation (CPA) theory to obtain an estimation of the elastic properties of the heavy oil sand. They match their results with the experimental data, which shows qualitative agreement. This theory was then further developed by Makarynska et al. (2010). Other researchers utilized the de la Cruz-Spanos theory (Eastwood, 1993) and the generalized Biot theory (Tsiklauri and Beresnev, 2003) to calculate the acoustic velocities of the heavy oil sand. All these models do not consider any specific heavy oil distribution, the heavy oil sand is treated as the general isotropic medium. These models may be applied well when several types of heavy oil distributions co-exist which results in the averaged values of the elastic moduli for the heavy oil sand. However, as pointed out by Han et al. (2007), the heavy oil usually has specific distributions which play a vital role on the elastic properties of the heavy oil sand. Hence, acoustic velocity models for the heavy oil sand should be built based on the heavy oil distribution.

Only a few models have considered the influences of heavy oil distributions. One such model was proposed by Leurer and Dvorkin (2000, 2006) for the heavy oil distributed at sand grain contacts, which acts as the viscoelastic cement in the heavy oil sand resulting in the frequency-dependent acoustic velocities and attenuations. To build the acoustic velocity models for the heavy oil sand, more heavy oil distribution types need to be taken into account. As the elastic properties of the heavy oil sand will both depend on the heavy oil distributions and frequency in the intermediate temperature, it is reasonable to establish the acoustic velocity models for the heavy oil sand in the low temperature first. Under this condition, the influences of the heavy oil distribution can be investigated conveniently without the effects of the frequencies. The acoustic velocity models for the heavy oil sand at the intermediate temperature can be developed in the future by incorporating the influences of the frequencies.

As observed by Han et al. (2007) in the experiments, the heavy oil in the low temperature has three primary distributions in the heavy oil sand (Fig. 1): a) the sands are water wet which makes the heavy oil detached from the pore walls, the heavy oil thus becomes part of the fluid. In this case, the heavy oil can only support the pore pressure, its influences on the acoustic velocities can be modelled in the similar way as the fluids. b) The heavy oil saturation is high enough that it forms the matrix, the sand grains thus float inside the matrix. c) The heavy oil has a relatively low saturation degree and accumulates at the grain contacts. The sands are cemented by the heavy oil which significantly increases the acoustic velocities of the heavy oil sand. The last two types of heavy oil distributions often occur for the oil wet sands. Depending on the different heavy oil distribution, different acoustic velocity model for the heavy oil sand should be built.

In this paper, we proposed the corresponding acoustic velocity model for the heavy oil sand under each specific heavy oil distribution in the low temperature (Fig. 1). Then the heavy oil sands from Xinjiang Oil Field of China are studied, the proper acoustic velocity model is selected based on its heavy oil distribution. Furthermore, the estimation results for other oil distributions are also given and analyzed based on the corresponding models. Finally, the potential applications of the acoustic velocity models are discussed.

2. Acoustic velocity models under different type of heavy oil distribution

The heavy oil in the low temperature behaves like an elastic solid. Therefore, the heavy oil sand under this condition also has the elastic properties, its compressional and shear wave velocities can thus be calculated from its moduli (bulk and shear moduli) and density as follows:

$$V_p = \sqrt{\frac{K_{eff} + 4/3G_{eff}}{\rho}}, \tag{1}$$

$$V_s = \sqrt{\frac{G_{eff}}{\rho}}, \tag{2}$$

where V_p and V_s are the compressional and shear wave velocities, respectively; K_{eff} and G_{eff} is the effective bulk and shear moduli of the heavy oil sand, respectively; ρ is the density of the heavy oil sand.

Thus, the bulk and shear moduli are needed to calculate the acoustic velocities of the heavy oil sand. Most current models, such as K-T model (Kuster and Toksoz, 1974), Self-Consistent theory (SC) (Berryman, 1980), and Differential Effective Medium (DEM) model (Berryman, 1992), are proposed for the consolidated sandstone. For the heavy oil sand in the low temperature, it is usually unconsolidated with very low acoustic velocities which can be easily overestimated by these models. Therefore, the models for the unconsolidated sandstones are required to estimate its acoustic velocities. To this end, some models have been developed, which mainly include Hertz-Mindlin (HM) model (Mindlin, 1949), Contact Cement Theory (CCT) (Dvorkin et al., 1994), and Hertz-Mindlin- Hashin-Shtrikman (HMHS) model (Dvorkin and Nur, 1996). Such models estimate the moduli of the sandstone from the

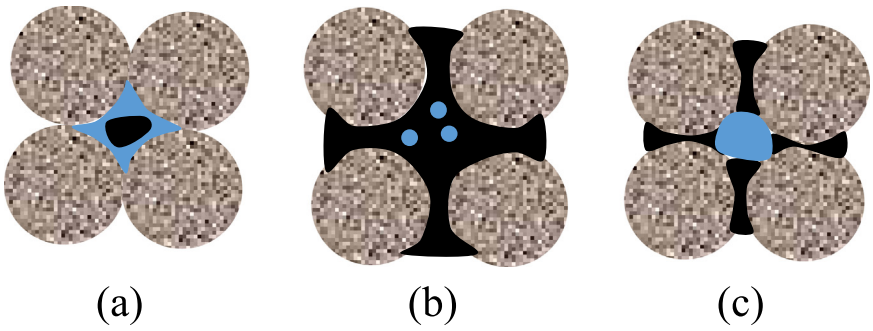

Fig. 1. Three types of oil distributions. (a) Heavy oil is part of the pore fluid. (b) Heavy oil forms the continuous matrix. (c) Heavy oil cements the sand grains. Note that the blue part represents formation water and the black part stands for the heavy oil. For Type a, the sand grains are usually water wet. For the other two types, the sand grains are normally oil wet. (For interpretation of the references to color in this figure legend, the reader is referred to the web version of this article.)

contact stiffness between the grains. They give much better estimation results for the acoustic velocities of the unconsolidated sandstone than the conventional models. These models are based on the microstructures of the unconsolidated sandstones, different microstructures correspond to different models. Therefore, the models should be selected according to the microstructures of the unconsolidated sandstone. The microstructure of the heavy oil sand is primarily controlled by the heavy oil distributions. It indicates that the acoustic velocity model for the heavy oil sand should be built based on the heavy oil distribution, which is consistent with the experimental observation made by Han et al. (2007). In the following text, we will propose appropriate models to calculate the moduli of the heavy oil sand in the low temperature for each type of oil distribution described in Fig. 1.

2.1. Models for Type a

For the first type of oil distribution, the heavy oil is detached from the water wet sand grains and is only part of pore fluid. Under this condition, the sand grains are usually held together by the pressure. The dry moduli of the sand matrix will be pressure dependent. Its values can be calculated by Hertz-Mindlin (HM) model (Mindlin, 1949), which are as follows:

$$K_d = \left[\frac{n^2(1-\phi)^2 G_0^2}{18\pi^2(1-\nu_0)^2}P\right]^{1/3} \tag{3}$$

$$G_d = \frac{5-4\nu_0}{5(2-\nu_0)}\left[\frac{3n^2(1-\phi)^2 G_0^2}{2\pi^2(1-\nu_0)^2}P\right]^{1/3} \tag{4}$$

where K_d and G_d are the bulk and shear moduli of the dry heavy oil sand, respectively; G_0 and ν_0 are the shear modulus and Poisson's ratio of the sand grains, respectively; Φ is the porosity of the heavy oil sand; n is the coordination number; P is the effective pressure applied on the heavy oil sand.

After the dry moduli of the heavy oil sand are obtained by Eqs. (3) and (4), the effective moduli of the heavy oil sand can be obtained after considering the fluid saturation effect. This effect can be calculated by Gassmann's formula as follows:

$$K_{eff} = K_d + \frac{(1-K_{dry}/K_0)^2}{\frac{\phi}{K_f} + \frac{1-\phi}{K_0} - \frac{K_d}{K_0^2}} \tag{5}$$

$$G_{eff} = G_d \tag{6}$$

where K_{eff} and G_{eff} are the bulk and shear moduli of the heavy oil sand saturated with heavy oil and the formation water; K_0 is the bulk modulus of the sand grains; K_f is the bulk modulus of the mixture of heavy oil and formulation water.

For the mixture of heavy oil and formulation water, Wood's (1955) formula can be used to obtain its bulk modulus:

$$K_f = \frac{1-S_w}{K_{oil}} + \frac{S_w}{K_w} \tag{7}$$

where S_w is the water saturation; K_{oil} and K_w are the moduli of the heavy oil and water, respectively.

Through Eqs. (3)–(7), the effective moduli of the heavy oil sand under this type of oil distribution can be obtained. Its velocities can then be calculated using Eqs. (1) and (2). However, Eqs. (3) and (4) are not suitable for the low porosity. For instance, Eqs. (3) and (4) show that the moduli of the heavy oil sand are still pressure dependent at zero porosity. This contradicts with the fact that the pressure has little influence on the moduli if the sandstone has zero porosity and is composed of pure sand grains. To solve this problem, the Hertz-Mindlin-Hashin-Shtrikman (HMHS) model (Dvorkin and Nur, 1996) originally developed for the unconsolidated sandstone can be used, in which the Hashin-Shtrikman (HS) lower bound (Hashin and Shtrikman, 1963) is used for the sandstone with porosities ranging from zero to the critical porosity with endpoints constrained by the bulk and shear moduli of the solid phase (zero porosity and hence pressure independent) and the moduli at the critical porosity is determined by the HM model. For the heavy oil sand, the formulas are as follows:

$$K_d = \left[\frac{\phi/\phi_0}{K_{HM}+4/3G_{HM}} + \frac{1-\phi/\phi_0}{K_0+4/3G_{HM}}\right]^{-1} - \frac{4}{3}G_{HM} \tag{8}$$

$$G_d = \left[\frac{\phi/\phi_0}{G_{HM}+\frac{G_{HM}}{6}z} + \frac{1-\phi/\phi_0}{G_0+\frac{G_{HM}}{6}z}\right]^{-1} - \frac{G_{HM}}{6}z \tag{9}$$

$$z = \frac{9K_{HM}+8G_{HM}}{K_{HM}+2G_{HM}} \tag{10}$$

where K_{HM} and G_{HM} are the bulk and shear moduli of the dry heavy oil sand at the critical porosity, respectively, which are calculated by the HM model; Φ_0 is the critical porosity; Φ is the porosity of the heavy oil sand; K_0 and G_0 are the bulk and shear moduli of the sand grains, respectively.

Fig. 2 shows the pressure dependence of the dry moduli of heavy oil sand, which is calculated by this model. It can be clearly seen that there is no pressure dependence at zero porosity and the moduli are equal to that of the solid phase. This proves that using the HMHS model enables us to estimate the moduli of the dry heavy oil sand at low porosity. In fact, Dvorkin and Nur (1996) has shown that HMHS model also gives good estimation results at the high porosity. Therefore, it is recommended that HMHS model

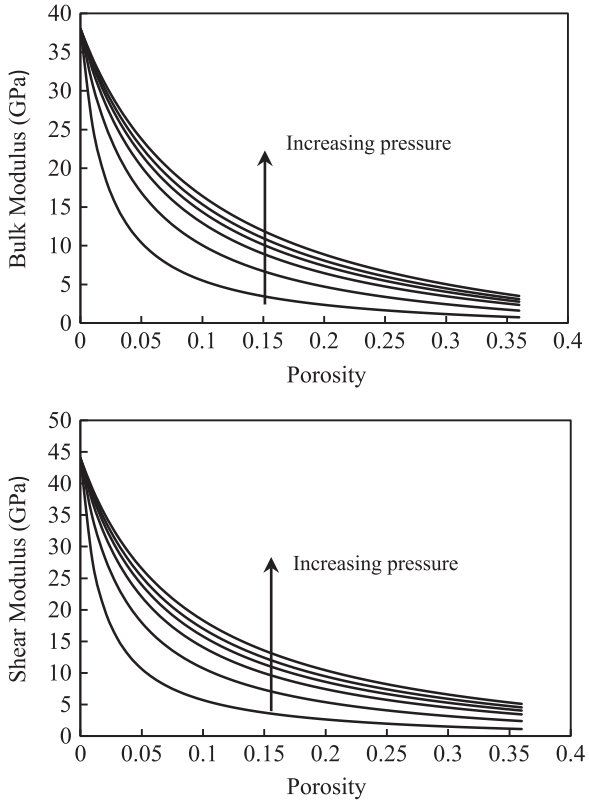

Fig. 2. The bulk and shear moduli variations with porosity under different effective pressures for the dry heavy oil sand. Note that the sand grains are pure quartz and the critical porosity used is 0.36. The results are calculated using HMHS model (Dvorkin and Nur, 1996).

should be used instead of HM model for both the high and low porosities.

2.2. Models for Type b

If the pore space is almost occupied by the heavy oil, a continuous matrix will be formed by the heavy oil and the sand grains will float inside the matrix. Under this condition, the HS lower bound can be used to calculate moduli of the heavy oil sand (Gurevich et al., 2007; Han et al., 2007). Since the matrix is composed of heavy oil and the inclusions are the sand grains, the HS lower bound for the heavy oil sand moduli has the following form:

$$K_{eff} = K_{oil} + \frac{1-\phi}{(K_0 - K_{oil})^{-1} + \phi(K_{oil} + 4/3G_{oil})}, \tag{11}$$

$$G_{eff} = G_{oil} + \frac{1-\phi}{(G_0 - G_{oil})^{-1} + \frac{2\phi(K_{oil}+2G_{oil})}{5G_{oil}(K_{oli}+4/3G_{oli})}}, \tag{12}$$

where K_{eff} and G_{eff} are the effective bulk and shear moduli of the heavy oil sand, respectively; K_{oil} and G_{oil} represent the bulk and shear moduli of the heavy oil, respectively; K_0 and G_0 are the bulk and shear moduli for the sand grains, respectively; Φ is the porosity of the heavy oil sand.

2.3. Models for Type c

If the heavy oil saturation is relative low, it can accumulates at the grain contacts. The sand grains can thus be cemented by the heavy oil, which significantly increases the elastic properties of the heavy oil sand. Therefore, cementation effects of the heavy oil on the sand grains under this condition must be considered. Up until now, only a few models have been proposed to analyze these effects. Among them, the most important and useful model is the Contact Cement Theory (CCT). This theory was developed by Dvorkin et al. (1994) to model the effects of cements on the normal and tangential stiffness of a grain-cement combination. The elastic properties of the sandstone can then be estimated. The applications of this theory on the samples obtained from Oseberg demonstrate its applicability for the unconsolidated sandstone with weak cementation (Dvorkin and Nur, 1996). However, it is found by Han et al. (2013, 2014) that the influences of the contact thickness, i.e., the minimal distance between two adjacent grains, on the normal and tangential stiffness are ignored in the CCT. As the existence of the contact thickness decreases the normal and tangential stiffness, the elastic moduli of the unconsolidated sandstone will thus decrease. Hence, the CCT will overestimate the acoustic velocities of the weakly cemented unconsolidated sandstone with the non-zero contact thickness. To take into account the effects of contact thickness, Han et al. (2013, 2014) modified the CCT to incorporate this parameter and validated the modified CCT using the experimental data. For the heavy oil acting as the cement, the sand grains often do not contact each other due to the low compaction rate at the shallow burial depth. Therefore, the contact thickness for this type of heavy oil sand is usually not zero and the modified CCT should be used to calculate its elastic moduli. The modified CCT is briefly introduced in the following.

The bulk and shear moduli of the heavy oil sand are obtained from the normal and tangential stiffness through the modified CCT as follows (Dvorkin et al., 1994; Han et al., 2013, 2014):

$$K_{eff} = \frac{G_{oil}(1-\nu_{oil})}{1-2\nu_{oil}} \frac{n(1-\phi_0)}{3(1+\varepsilon)} S_n \tag{13}$$

$$G_{eff} = \frac{3}{5}K_{eff} + \frac{3G_{oil}n(1-\phi_0)}{20(1+\varepsilon)} S_\tau \tag{14}$$

where K_{eff} and G_{eff} are the bulk and shear moduli of the heavy oil sand, respectively; G_{oil} and ν_{oil} are the shear modulus and Poisson's ratio of the heavy oil cement, respectively; S_n and S_τ represent the normal and tangential stiffness, respectively; Φ_0 is the critical porosity; n is the coordination number; ε is the contact thickness, which is the ratio of the minimal half distance between two adjacent grains, h, to the radius of the grains, R.

The parameters for normal and tangential stiffness, S_n and S_τ, are determined by the cement amount, the contact thickness, and the properties of the grains and heavy oil cement. The calculations of these two parameters based on the rigorous theory require the numerical approach which is time consuming. Hence, we computed their values in a large scale of elastic properties of the sands and cements, and also for different contact thickness and cement amount. Based on this, a good statistical approximation for them are proposed, which is shown in Appendix. The cement amount is quantified by the cementation radius, α, which is defined as the ratio of the heavy oil cement layer, a, to the radius of the grain, R. For the heavy oil accumulating at the grain contacts (Fig. 3a), α is influenced by the contact thickness and is as follows (Han et al., 2013, 2014):

$$\alpha = \sqrt{-2\varepsilon + 2\sqrt{\varepsilon^2 + \frac{4}{3n}\frac{\phi_0 - \phi}{1-\phi_0}}} \tag{15}$$

Apart from the grain contacts, the heavy oil cement may also distribute at the other parts of the sand. For instance, the cement can evenly distribute on the grain surface (Fig. 3b). The expression for the cementation radius under this condition is independent of the contact thickness and has the following form (Han et al., 2013, 2014):

$$\alpha = \sqrt{\frac{2(\phi_0 - \phi)}{3(1-\phi_0)}} \tag{16}$$

Thus, through the modified CCT, the dry moduli of this type of heavy oil sand can be calculated. If the heavy oil sand is saturated with the fluids, Gassmann's formula can be used to calculate the fluid saturation effect, as shown before.

The elastic properties for these three types of heavy oil sand can thus be calculated through the corresponding models. The acoustic velocities can then be obtained using Eqs. (1) and (2).

3. Application of the models

In this section, the acoustic velocities data of heavy oil sand from Xinjiang Oil Field of China are analyzed by the models proposed above. The sand grains are mainly composed of quartz, with the bulk and shear moduli to be 38 GPa and 44 GPa. The thin section image shows that the sand grains are cemented by the

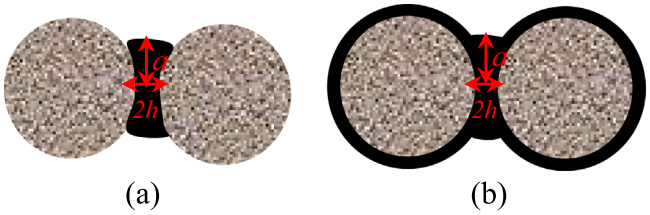

Fig. 3. Schemes for the distributions of the heavy oil cement in the heavy oil sand. (a) Heavy oil only accumulates at the grain contacts. (b) Apart from the heavy oil in the grain contacts, the heavy oil also distributes evenly on the grain surface. Note that the minimal distance between two grains ($2h$) is not zero.

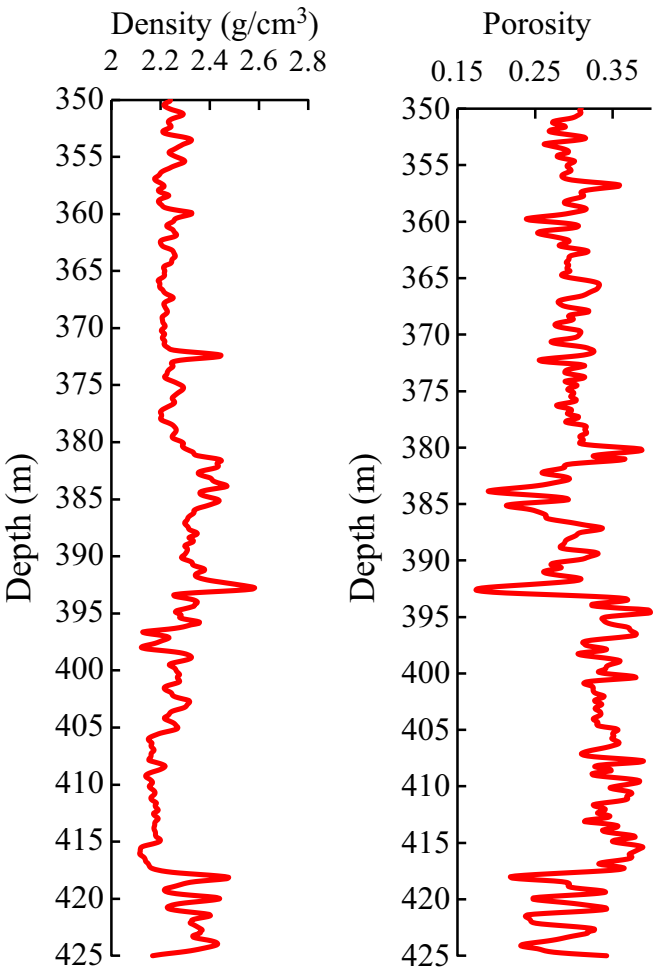

Fig. 4. Varying densities and porosities of the heavy oil sand with depth.

heavy oil at the grain contacts. Most of the sand grains do not contact each other, there is a contact thickness between two grains. By measuring the radius of the sand grains and the thickness of the heavy oil cement, the contact thickness, ϵ, is estimated to be around 0.015. Based on this fact, these heavy oil sands belong to Type c, the modified CCT should be used. The temperature at the depth of the heavy oil sand formation (350–425 m) is close to 20 °C. At such temperature, the bulk and shear moduli of the heavy oil is about 3.4 GPa and 0.9 GPa, based on Batzle's measurement (Batzle et al., 2004). As the heavy oil mainly accumulates at the grain contacts, we use the first Scheme to calculate the cementation radius (Eq. (15)). The density and porosity of the heavy oil sand change with the depth, which are shown in Fig. 4. According to the distribution of the porosity, the critical porosity is assumed to be 40%, with the coordination number to be 8.5. Using these parameters, the dry moduli of the heavy oil sand can be calculated using the modified CCT. As the heavy oil sand is saturated with formation water, the fluid saturation effect also needs to be considered. The Gassmann's formula can be used with the bulk modulus of the formation water to be 2.7 GPa. The estimation results are shown in Figs. 5 and 6. Fig. 5 shows the measured and predicted velocities versus the depth, whereas Fig. 6 compares the measured and predicted velocity values through the crossplots. To illustrate the influence of the contact thickness, the results with zero contact thickness are also shown in these two figures.

Figs. 5 and 6 show that without considering the influence of contact thickness, both the compressional and shear wave velocities will be largely overestimated. The reason for the

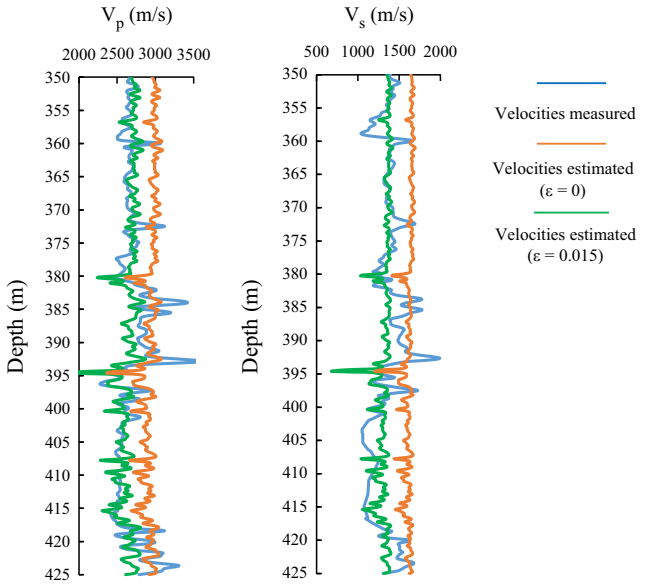

Fig. 5. Measured and predicted velocities versus depth. The velocities are predicted using modified CCT with and without considering the influence of contact thickness.

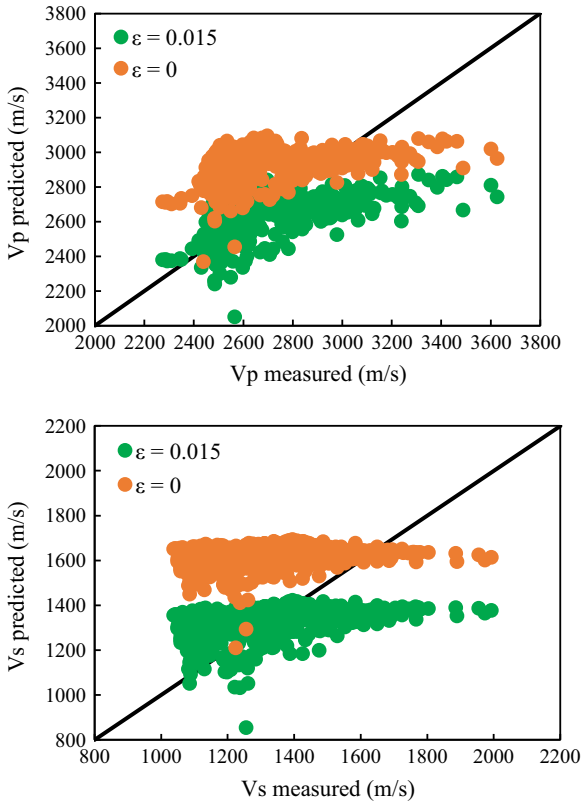

Fig. 6. Predicted velocities versus measured velocities. The velocities are predicted using modified CCT with and without considering the influence of contact thickness.

overestimation is that the existence of the contact thickness reduces the normal and tangential stiffness. As a result, the moduli and the acoustic velocities of the heavy oil sand will decrease. Therefore, it is crucial to take into account the influence of contact thickness when estimating the acoustic velocities of the heavy oil sand. Through applying the modified CCT which considers the contact thickness effects, the discrepancies between the measured and predicted values are reduced significantly (from 11% to 4%).

Furthermore, the correlation coefficient between the measured and predicted values increases from 0.35 to 0.65. Given the complexity of the well logging measurement environment compared with that of the lab, this improvement in correlation coefficient should be considered to be good. It is also found that the modified CCT tends to underestimate the high values of measured compressional wave velocities which correspondences to the relative low porosities, the possible reason is that not only heavy oil but also other cements (such as clays) may exist in the pore space when the porosity is relatively low. The cementation effects of the other cements are not considered in our model, therefore, the velocities are underestimated. In general, the modified CCT gives good predictions of the compressional wave velocities of this data set.

For the prediction results of the shear wave velocities, they are not as good as the compressional wave velocities. While the discrepancies between the measured and predicted shear wave velocities are also reduced significantly (from 22% to 8%), the correlation coefficient doesn't increase and is very low (about 0.30). This indicates that the shear wave velocities decrease almost linearly with the contact thickness, which results in the nearly constant shift of the shear wave velocities towards the lower values with the increasing contact thickness. Moreover, it is also noted that the predicted shear wave velocities changes little with the depth, whereas the measured data varies more obviously with the depth. This leads to the low correlation coefficient between the measured and predicted shear wave velocities. Dvorkin and Nur (1996) shows that the shear wave velocities of the unconsolidated sandstone with weak cementation are not sensitive to porosities when the porosities are obviously smaller than the critical porosity. In this case, most porosities at this depth interval vary between 0.25 and 0.30, which are obviously smaller than the critical porosity (0.40). Hence, our prediction of shear wave velocities keeps nearly constant, which are consistent with those observed by Dvorkin and Nur (1996). The obvious variation of the measured shear wave velocities may be due to the poor recordings of the shear waves which result from the high attenuation of shear wave energies. On the whole, it is reasonable to conclude that the modified CCT gives good prediction results for this set of acoustic velocity data for which the sands are cemented by the heavy oil.

Here, it should be noted that the modified CCT currently does not take into account the velocity changes with varying effective pressure (Dvorkin et al., 1994; Han et al., 2014). As the cement is loading bearing, the cement-grain combination acts as an elastic body with the pressure independent elastic constants. This assumption may not work well for the sandstones with cracks, as the increase of the effective pressure will close the cracks and increase the velocities of the sandstone. However, this assumption is valid for the heavy oil sand. This is because the heavy oil sand is usually buried at the shallow depth with low effective pressure, there is nearly no cracks developed in the heavy oil sand. This can be validated by the porosity data (Fig. 4), which shows no dependence on the depth (effective pressure). In this case, the effective pressure for this heavy oil sand formation is around 5 MPa, the velocities are estimated well by the modified CCT.

If we assume that the heavy oil is distributed as Type a or b, the HMHS model or HS lower bound can be applied to estimate the acoustic velocities. To compare the estimation results for different heavy oil distributions, the estimation results for this set of data using the HMHS model and HS lower bound are compared in Figs. 7 and 8 (using depth and cross plots respectively), together with the results by the modified CCT ($\varepsilon=0.015$).

The effective pressure used in the HMHS model is calculated using the density log data. The other parameters are the same with the parameters used in the modified CCT. It is found that HMHS model underestimates both the compressional and shear wave

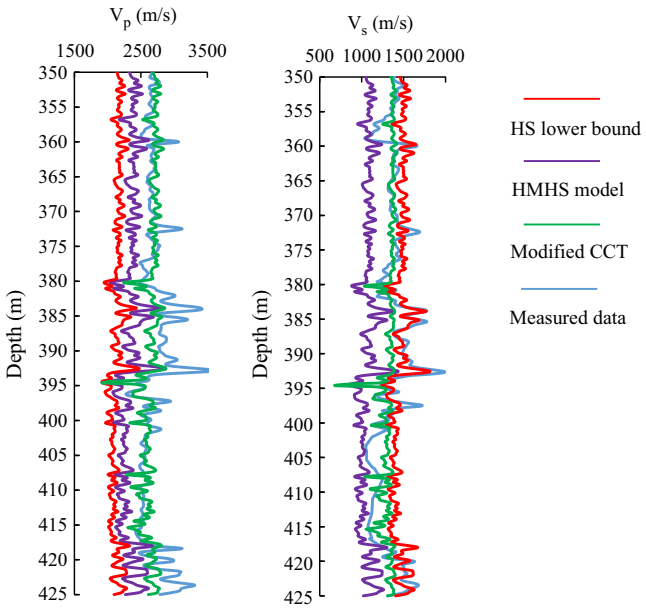

Fig. 7. Measured and predicted velocities versus depth. The velocities are predicted using three models, HMHS, HS lower bound, and modified CCT ($\varepsilon=0.015$).

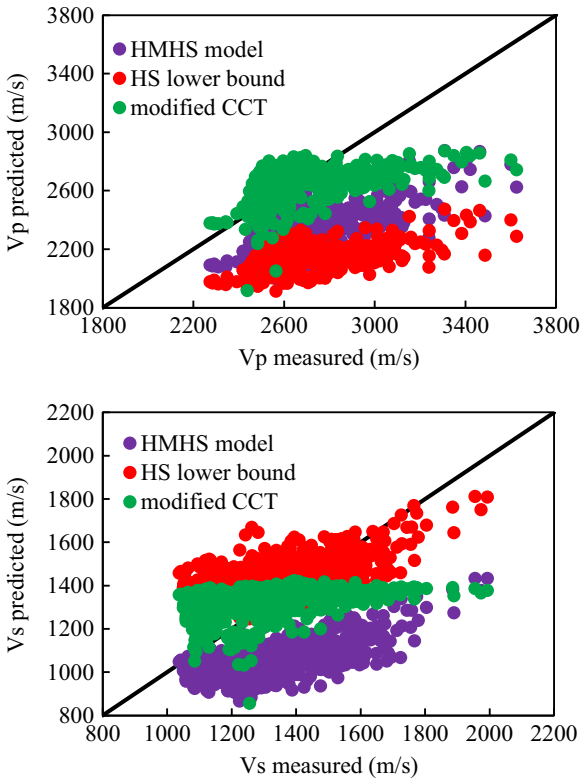

Fig. 8. Measured velocities versus predicted velocities. The velocities are predicted using three models, HMHS, HS lower bound, and modified CCT ($\varepsilon=0.015$).

velocities. This indicates that the sand grains are not only held together by the effective pressure, they are also bounded by the heavy oil at the grain contacts. Although the content of the heavy oil cement is not high, it can significantly increase the stiffness of the heavy oil sand. As a result, the compressional and shear wave velocities will increase. This effect is well described by the modified CCT. For the HS lower bound, it is interesting to find that this bound estimates the much lower compressional wave velocities than the modified CCT, but it gives a close estimation for the shear

wave velocities compared with those given by the modified CCT. This can be explained by the assumptions of the models. The HS lower bound assumes that the heavy oil forms the continuous matrix with the sand grains floating inside. Therefore, the moduli for this type of heavy oil sand are largely determined by those of the heavy oil. The modified CCT is based on the grain-heavy oil cement combination (Fig. 3). The moduli of the heavy oil sand are primarily decided by the stiffnesses of the grain-heavy oil cement combination. Under this condition, the compressional modulus depends on the moduli of the sand grains, whereas the shear modulus is decided by the shear modulus of the heavy oil cement. As the moduli of the sand grains are much higher than those of the heavy oil, the compressional wave velocities estimated by the modified CCT will be much larger than those estimated by the HS lower bound. However, the shear wave velocities estimated by the modified CCT and the HS lower bound are both determined by the shear modulus of the heavy oil. This results in the similar estimation results of the shear wave velocities by the modified CCT and the HS lower bound. Here, it should be noted that while the prediction results of the shear wave velocities given by the HS lower bound seem to have higher correlation coefficient with the measured data (about 0.6) than those given by the modified CCT (about 0.3) in this case, it doesn't mean that the HS lower bound can predict shear wave velocities better than the modified CCT for the sands cemented by the heavy oil. The reason is that the quality of the measured shear wave velocity data may be poor, which makes the measured data deviate from the real values, as discussed before.

4. Discussions

The analysis above shows that the estimation results by the models are based on the distributions of the heavy oil. This fact implies that the microstructures (or the heavy oil distributions) of the heavy oil sand can be studied by matching the measured acoustic velocities data with the estimation results by the models. Each model corresponds to one type of the heavy oil distributions, the model that matches the measured data best implies the primary heavy oil distribution in the sand.

Once the heavy oil distribution is known, many properties of the sand can be obtained. For example, the strength of the heavy oil sand can be estimated. Yin and Dvorkin (1994) and Dvorkin and Nur (1996) show that the sand grains can be prevented from breaking at the high pressure by even a small amount of cement. Therefore, if sand grains are cemented by the heavy oil at the grain contacts, the heavy oil sand is mechanically stable and sanding is unlikely. In contrary, if sand grains are kept together through the confining pressure, the sand could be mechanically unstable and the sanding may occur with the release of the confining pressure. It is important to mention that we only discuss the solid phase of the heavy oil in the low temperature here. During the thermal recovery, the increase of the temperature will make the heavy oil transfer to the liquid phase. The heavy oil would not be able to cement the sand grains or form the continuous matrix. Thus, the strength of heavy oil sand for Type b and c will decrease greatly and the chance of sanding will be much higher. Apart from estimating the mechanical strength, the heavy oil distribution also help us gain understanding on the other properties, such as the permeability.

5. Conclusions

We have proposed the acoustic velocity models for the heavy oil sand with different oil distribution in this paper. There are primary three types of oil distributions in the heavy oil sand. For the first type, the oil is detached from the water wet sand grains and is only part of the pore fluid. The confining pressure holds the sand grains together. Under this condition, the HMHS model can be used for the acoustic velocities prediction. In the second type, the heavy oil has high saturation which forms the matrix. The sand grains act as the inclusions that float in the heavy oil matrix. Therefore, the HS lower bound should be applied in the velocities prediction. For the third type, the heavy oil acts as the cement. The sand grains are cemented by the heavy oil at the grain contacts. This cementation effect can be described well by the modified CCT. Thus, this model can be applied for this type of heavy oil sand.

To validate the proposed models, the oil distribution for the heavy oil sand of Xinjiang Oil Field is studied. Based on its oil distribution, the modified CCT is selected and the good estimation results are obtained. To compare the results for different oil distributions, the estimation results using HMHS and the HS lower bound are also given. The results show that different heavy oil distribution results in different acoustic velocities responses. The heavy oil distribution can be obtained by matching the measured data with the estimation results by different models. The model that match the data best implies the primary oil distribution. Once the heavy oil distribution is known, many properties of the sand can be estimated, such as the strength and the permeability.

Acknowledgments

We would like to thank the financial support from National Natural Science Foundation of China, Contract U1562108, and the data provided by Xinjiang Oil Field of China.

Appendix. Computation of S_n and S_τ

Parameters S_n and S_τ in Equations 13 and 14 are:

$$S_n = A_n(\Lambda_n, \varepsilon)\alpha^2 + B_n(\Lambda_n, \varepsilon)\alpha + C_n(\Lambda_n, \varepsilon),$$

$$S_\tau = A_\tau(\Lambda_\tau, \varepsilon)\alpha^2 + B_\tau(\Lambda_\tau, \varepsilon)\alpha + C_\tau(\Lambda_\tau, \varepsilon),$$

where

For Λ_n: 0.007 – 0.04:

If $\varepsilon \le 0.008$:

$$A_n = -(6216.7\varepsilon^2 - 22.783\varepsilon + 0.1646)\Lambda_n^{(13667\varepsilon^2 - 55.333\varepsilon - 0.658)}$$

$$B_n = (9916.7\varepsilon^2 - 35.883\varepsilon + 0.5643)\Lambda_n^{(6166.7\varepsilon^2 - 25.833\varepsilon - 0.514)},$$

$$C_n = -(-183.33\varepsilon^2 - 0.5833\varepsilon - 0.0037)\Lambda_n^{(12667\varepsilon^2 + 132.67\varepsilon - 1.112)}$$

Otherwise:

$$A_n = -(-43\varepsilon^2 + 8.5493\varepsilon + 0.1451)\Lambda_n^{(2.381\varepsilon^2 + 14.445\varepsilon - 0.7159)}$$

$$B_n = (-276.67\varepsilon^2 + 24.839\varepsilon + 0.4696)\Lambda_n^{(-95.238\varepsilon^2 + 11.605\varepsilon - 0.5706)};$$

$$C_n = -(-9.2381\varepsilon^2 + 1.8876\varepsilon - 0.0145)\Lambda_n^{(-472.38\varepsilon^2 + 38.719\varepsilon - 1.1876)}$$

For Λ_n: 0.04 – 0.20:

If $\varepsilon \le 0.008$:

$$A_n = -(71.985\varepsilon^2 - 0.2727\varepsilon + 0.0468)\Lambda_n^{(1172.1\varepsilon^2 - 9.5666\varepsilon - 1.0511)}$$

$$B_n = (274.87\varepsilon^2 - 2.2312\varepsilon + 0.2667)\Lambda_n^{(726.13\varepsilon^2 - 7.4196\varepsilon - 0.748)},$$

$$C_n = -(-8.9196\varepsilon^2 + 0.1629\varepsilon - 0.0014)\Lambda_n^{(13629\varepsilon^2 + 6.8405\varepsilon - 1.4379)}$$

Otherwise:

$$A_n = -(5.7792\varepsilon^2 + 0.4569\varepsilon + 0.0446)\Lambda_n^{(105.71\varepsilon^2+5.3505\varepsilon-1.1159)}$$
$$B_n = (0.2771\varepsilon^2 + 1.928\varepsilon + 0.2462)\Lambda_n^{(19.307\varepsilon^2+3.3416\varepsilon-0.8023)} \quad ;$$
$$C_n = -(0.3939\varepsilon^2 + 0.2114\varepsilon - 0.0018)\Lambda_n^{(-283.46\varepsilon^2+31.128\varepsilon-1.7754)}$$

For Λ_n: 0.20 – 0.65:
If $\varepsilon \le 0.005$:

$$A_n = -(-100\varepsilon^2 + 0.76\varepsilon + 0.0289)\Lambda_n^{(-1250\varepsilon^2+7.65\varepsilon-1.3789)}$$
$$B_n = (-75\varepsilon^2 + 0.635\varepsilon + 0.2069)\Lambda_n^{(-\varepsilon-0.907)} \quad ,$$
$$C_n = -(0.2\varepsilon - 0.001)\Lambda_n^{(11500\varepsilon^2-2.3\varepsilon-1.4673)}$$

Otherwise:

$$A_n = -(-1.2987\varepsilon^2 + 0.0066\varepsilon + 0.0314)\Lambda_n^{(91.429\varepsilon^2+0.701\varepsilon-1.3726)}$$
$$B_n = (-0.6926\varepsilon^2 + 0.1082\varepsilon + 0.2083)\Lambda_n^{(23.506\varepsilon^2+0.2463\varepsilon-0.9181)} \quad ;$$
$$C_n = -(-0.6277\varepsilon^2 + 0.12\varepsilon - 0.0005)\Lambda_n^{(-57.619\varepsilon^2+9.9538\varepsilon-1.7214)}$$

For Λ_τ: 0.0007 – 0.014:
If $\varepsilon \le 0.004$:

$$A_\tau = -(-189200\varepsilon^2 + 659.2\varepsilon + 0.5819)\Lambda_\tau^{(-45500\varepsilon^2+148.5\varepsilon-0.389)}$$
$$B_\tau = (-151900\varepsilon^2 + 622.1\varepsilon + 1.7838)\Lambda_\tau^{(-15000\varepsilon^2+56\varepsilon-0.271)} \quad ,$$
$$C_\tau = -(21000\varepsilon^2 - 69.8\varepsilon - 0.0269)\Lambda_\tau^{(-95000\varepsilon^2+423\varepsilon-0.688)}$$

Otherwise:

$$A_\tau = -(124.33\varepsilon^2 - 30.79\varepsilon + 1.9189)\Lambda_\tau^{(-109.21\varepsilon^2+0.5713\varepsilon-0.1583)}$$
$$B_\tau = (-407.4\varepsilon^2 + 1.1729\varepsilon + 3.2628)\Lambda_\tau^{(-51.498\varepsilon^2+5.2906\varepsilon-0.1819)} \quad ;$$
$$C_\tau = -(-147.98\varepsilon^2 + 11.199\varepsilon - 0.018)\Lambda_\tau^{(-128.33\varepsilon^2+11.621\varepsilon-0.3323)}$$

For Λ_τ: 0.014 – 0.18:
If $\varepsilon \le 0.008$:

$$A_\tau = -(766.67\varepsilon^2 - 2.8333\varepsilon + 0.0686)\Lambda_\tau^{(5666.7\varepsilon^2-26.333\varepsilon-0.914)}$$
$$B_\tau = (1850\varepsilon^2 - 8.65\varepsilon + 0.3322)\Lambda_\tau^{(2666.7\varepsilon^2-15.333\varepsilon-0.669)} \quad ,$$
$$C_\tau = (-16.667\varepsilon^2 - 0.0167\varepsilon + 0.0018)\Lambda_\tau^{(9833.3\varepsilon^2+65.833\varepsilon-1.324)}$$

Otherwise:

$$A_\tau = -(4.8571\varepsilon^2 + 1.5429\varepsilon + 0.0625)\Lambda_\tau^{(71.905\varepsilon^2+10.283\varepsilon-0.9905)}$$
$$B_\tau = (-29.81\varepsilon^2 + 5.4562\varepsilon + 0.2946)\Lambda_\tau^{(-18.571\varepsilon^2+6.9643\varepsilon-0.7339)};$$
$$C_\tau = -(0.381\varepsilon^2 + 0.3952\varepsilon - 0.0032)\Lambda_\tau^{(-445.71\varepsilon^2+39.143\varepsilon-1.6059)}$$

For Λ_τ: 0.18 – 0.32:
If $\varepsilon \le 0.005$:

$$A_\tau = -(0.2\varepsilon + 0.0357)\Lambda_\tau^{(500\varepsilon^2-4.9\varepsilon-1.2729)}$$
$$B_\tau = 0.2259\Lambda_\tau^{(500\varepsilon^2-4.1\varepsilon-0.8691)} \quad ,$$
$$C_\tau = -(25\varepsilon^2 - 0.245\varepsilon + 0.0009)\Lambda_\tau^{(9250\varepsilon^2+0.95\varepsilon-1.5826)}$$

Otherwise:

$$A_\tau = -(-0.1212\varepsilon^2 + 0.0579\varepsilon + 0.0366)\Lambda_\tau^{(125.63\varepsilon^2+1.4357\varepsilon-1.304)}$$
$$B_\tau = (1.1775\varepsilon^2 + 0.3014\varepsilon + 0.2234)\Lambda_\tau^{(29.784\varepsilon^2+0.8197\varepsilon-0.8939)} \quad ;$$
$$C_\tau = -(-0.4675\varepsilon^2 + 0.1367\varepsilon - 0.0006)\Lambda_\tau^{(-51.472\varepsilon^2+11.578\varepsilon-1.6762)}$$

$$\Lambda_n = \frac{2G_c}{\pi G}\frac{(1-\nu)(1-\nu_c)}{1-2\nu_c},\ \Lambda_\tau = \frac{G_c}{\pi G},\ \alpha = \frac{a}{R}.$$

In the above equations, ν_{oil} and G_{oil} are the Poisson's ratio and shear modulus of the heavy oil, respectively; ν and G are the Poisson's ratio and shear modulus of the sand grains, respectively; ε is the ratio of the contact thickness, h, to the radius of the grain, R; α is the ratio of the cementation radius, a, to the radius of the grain, R.

These equations for S_n and S_τ are approximated statistically from the theoretical solutions (Dvorkin et al, 1994; Han et al., 2014). The correlation between the rigorous solutions and the approximations is above 0.98 and the error is less than 3%.

References

Batzle, M., Hofmann, R., Han, D.-H., 2004, Heavy oils- seismic properties: 74th Annual International Meeting, SEG, Expanded Abstracts, pp. 1762 –1765.
Berryman, J.G., 1980. Long-wavelength propagation in composite elastic media. J. Acoust. Soc. Am. 28, 179–191.
Berryman, J.G., 1992. Single-scattering approximations for coefficients in Biot's equations of poroelasticity. J. Acoust. Soc. Am. 91, 551–571.
Das, A., Batzle, M., 2008. Modeling studies of heavy oil-in between solid and fluid properties. Lead. Edge 27 (9), 1116–1123.
Dvorkin, J., Nur, A., 1996. Elasticity of high-porosity sandstones: theory for two North Sea data sets. Geophysics 61 (5), 1363–1370.
Dvorkin, J., Nur, A., Yin, H., 1994. Effective properties of cemented granular materials. Mech. Mater. 18, 351–366.
Eastwood, J., 1993. Temperature-dependent propagation of P- and S- waves in Cold Lake oil sands: comparison of theory and experiment. Geophysics 58 (6), 863–872.
Gassmann, F., 1951, Über die Elastizität poroser medien: Veirteljahrsschrift der Naturforschenden Gesellschaft in Zürich, 96, pp. 1–23.
Gurevich, B., Osypov, K., Ciz, R., 2007, Viscoelastic modelling of rocks saturated with heavy oil: 77th Annual International Meeting, SEG, Expanded Abstracts, pp. 1614–1618.
Gurevich, B., Osypov, K., Ciz, R., Makarynska, D., 2008. Modeling elastic wave velocities and attenuation in rocks saturated with heavy oil. Geophysics 73 (4), E115–E122.
Han, D-H., Liu, J., Batzle, M., 2006, Acoustic property of heavy oil- measured data: 76th Annual International Meeting, SEG, Expanded Abstracts, pp. 1903–1907.
Han, D-H., Liu, J., Batzle, M., 2008, Velocity and dispersion of heavy oils: 77th Annual International Meeting, SEG, Expanded Abstracts, pp. 1690–1693.
Han, D-H., Yao, Q., Zhao, H.-Z., 2007, Complex properties of heavy oil sand: 77th Annual International Meeting, SEG, Expanded Abstracts, pp. 1609–1613.
Han, X., Guo, J., Li, F., Yang, L., Tang, J., 2013. Modified acoustic velocity model for basal cemented loose sandstone based on contact cement theory. J. China Univ. Pet. 37 (4), 76–82.
Han, X., Guo, J., Li, F., Yang, L., 2014. Generalization of the expression of cementation radius in Contact Cement Theory and its application. Chin. J. Geophys. 57 (7), 2235–2243.
Hashin, Z., Shtrikman, S., 1963. A variational approach to the elastic behaviour of multiphase materials. J. Mech. Phys. Solids 11, 127–140.
Kuster, G.T., Toksoz, M.N., 1974. Velocity and attenuation of seismic waves in two-phase media: part I, theoretical formulations. Geophysics 39 (5), 587–606.
Leurer, K.C., Dvorkin, J., 2000. Intergranular squirt flow in sand: grains with viscous cement. Int. J. Solids Struct. 37, 1133–1144.
Leurer, K.C., Dvorkin, J., 2006. Viscoelasticity of precompacted unconsolidated sand with viscous cement. Geophysics 71 (2), T31–T40.
Makarynska, D., Gurevich, B., Behura, J., Batzle, M., 2010. Fluid substitution in rocks saturated with viscoelastic fluids. Geophysics 75 (2), E115–E122.
Marion, D., Nur, A., 1991. Pore-filling material and its effects on velocity in rocks. Geophysics 56 (2), 225–230.
Mindlin, R.D., 1949. Compliance of elastic bodies in contact. J. Appl. Mech. 16, 259–268.
Speight, J.G., 2013. Heavy Oil Production Processes. Elsevier Inc, Waltham.
Tsiklauri, D., Beresnev, I., 2003. Properties of elastic waves in a non-Newtonian (Maxwell) fluid-saturated porous medium. Transp. Porous Media 53, 39–50.
Wolf, K., Mukerji, T., Mavko, G. 2006, Attenuation and velocity dispersion modelling of bitumen saturated sand: 76th Annual International Meeting, SEG, Expanded Abstracts, pp. 1993–1997.
Wood, A.W., 1955. A Textbook of Sound. Mcmillan Co, New York.
Yin, H., Dvorkin, J., 1994. Strength of cemented grains. Geophys. Res. Lett. 21, 903–906.